Icarus **145**, 580–590 (2000)
doi:10.1006/icar.2000.6348, available online at http://www.idealibrary.com on IDEAL®

The Buildup of a Tightly Bound Comet Cloud around an Early Sun Immersed in a Dense Galactic Environment: Numerical Experiments

Julio A. Fernández

Departamento de Astronomía, Facultad de Ciencias, Iguá 4225, 11400 Montevideo, Uruguay
E-mail: julio@fisica.edu.uy

and

Adrián Brunini

Facultad de Ciencias Astronómicas y Geofísicas, Universidad Nacional de La Plata, 1900 La Plata, Argentina—CONICET

Received May 12, 1998; revised January 3, 2000

We simulate numerically the buildup of a comet reservoir around the early Sun assumed to be still immersed in the placental molecular gas that gave birth to it, and to be gravitationally bound to other young stars formed out of the same gas. We show that under certain reasonable assumptions about the early galactic environment of the Sun, an inner core of the Oort cloud of radius from a few 10^2 AU to a few 10^3 AU forms on a time scale of a few million year. Jupiter and Saturn are the main scatterers of matter to this inner core, though a significant fraction of the matter scattered by these two planets (perhaps more than 50%) might originally come from the accretion zones of Uranus and Neptune. If the formation process of the jovian planets left unaccreted an amount of solid material of the same order of their own planet masses (the rock-icy cores for the cases of Jupiter and Saturn), then a few $M_\oplus$ of the scattered solid material might have been trapped in the Oort reservoir, most of it in the inner core.

Key Words: **comets; dynamics; origin.**

1. INTRODUCTION

Comets are probably the icy remnants of the planetary formation that were stored at large heliocentric distances by a combination of planetary and external perturbations. This concept is the basis of the theory developed by Oort (1950), who thought that passing stars were able to raise the perihelia of the scattered planetesimals above the planetary region, where they would remain until other stars would re-inject their perihelia into the planetary region or eject the bodies to interstellar space. Afterward, Byl (1983) showed that the tidal force of the galactic disk had actually a greater effect in driving perihelia of near-parabolic bodies out and into the planetary region. Yet, it was not until recently that the issue of the galactic environment of the early Sun was raised in connection with the buildup of the Oort comet cloud. An early reference to this idea can be found in Mottman (1977), who argued that the Sun was a member of an open cluster for several 10^8 year, so a very close encounter at low relative velocity with other cluster stars was very likely to occur triggering a comet shower responsible for the late heavy bombardment of the terrestrial planets.

Near-infrared observations of star-forming regions strongly argue in favor of the idea that stars usually form in clusters in dense regions ("cores") of molecular clouds of typical densities 10^4–10^5 H_2 cm^{-3} (e.g., Lada *et al.* 1993, 1996). Radio and infrared observations show that star clusters formed in such dense cores exhibit varying degrees of richness, ranging from a few members to several hundreds of stars. Indeed, within 500 pc of the Sun at least 90% of all stars younger than 10–15 Myr formed within four major associations, Scorpius-Centaurus, Perseus OB2, Orion OB1, and the Lacerta OB1 association (e.g., Bally *et al.* 1998). If we assume that the star formation efficiency within a core of 10^5 H_2 cm^{-3} is of 30% (the rest of the gas dissipates once the stars form) and allow for an expansion of the formed star cluster by a factor of three in size (Heller 1993), we obtain number densities of $\sim$25 stars pc^{-3} for stars of mass $\sim$1 $M_\odot$. Assuming virial equilibrium, cluster stars will have relative velocities $\sim$1 km s^{-1}, which are about 30 times smaller than the encounter velocities of the Sun with stars of its neighborhood at present.

One may question whether the Sun could have formed in such dense and harsh surroundings, where ultraviolet radiation from massive stars is able to strip away circumstellar envelopes of forming stars on time scales shorter than 10^5 year (Bally *et al.* 1998, Reipurth *et al.* 1998). Yet, O'Dell (1998) finds that proplyds (i.e., flattened circumstellar clouds of dust and gas surrounding stars collapsing toward the main sequence) in the Orion Nebula are more compact than the r^{-3} relation expected for a freely expanding gas, which argues in favor of a not-so-rapid loss of material from these objects. According to O'Dell, a constraining force provided by radiation pressure of Lyman-α

0019-1035/00 $35.00

photons, acting on the dust particles mixed with the proplyd gas, is responsible for slowing down the mass loss. Bally *et al.* (1998) also discussed the possibility that massive stars spend a substantial fraction of their lives embedded in an ultracompact HII region during which much of the stellar Lyman continuum radiation remains trapped close to the star. If planet embryos form fast enough in protoplanetary disks, say within 10^6 year, in that case formation of planetary systems should be compatible with Orion-like environments (Bally *et al.* 1998). This issue no doubt requires further study in order to set constraints on possible galactic environments of the early Sun.

Of course we cannot ascertain whether the Sun formed and remained for a certain time within a star cluster, like the one described before. Yet certain anomalous features of the current Solar System give some support to this hypothesis. For instance, Reeves (1978) suggested that a supernova explosion that occurred nearby, while the early solar nebula was still in its contracting phase, was responsible for the isotopic anomalies of oxygen and magnesium observed in several classes of meteorites. According to Reeves such a close supernova explosion was likely to occur only if the early Sun belonged to an OB association where the most massive members, after a fast evolution, ended up as supernovae. The tilt of about 7° of the Sun's spin axis with respect to the total angular momentum vector of the Solar System was explained by Mottman (1977) by torques on the orbital planes of the jovian planets produced by the same cluster star that caused the late heavy bombardment. Heller (1993) worked further on the idea of torques within star clusters. For a typical star cluster he found that torques on a protoplanetary disk, able to produce tilts of about 7° with respect to the spin axis of the central star, were possible for up to 40% of the cluster stars over a time scale of 1 Myr.

The other question of relevance is whether the scattering of the residual unaccreted bodies by the jovian planets occurred while the Sun was still in its natal environment. This question has been discussed by Fernández (1997, 1999) and Fernández and Brunini (1998), who argue that the answer is probably affirmative for Jupiter and Saturn, while it is more uncertain for Uranus and Neptune since the dynamical time scales for scattering involved are of several tens Myr. Yet a large number of the residual bodies scattered from the accretion zones of Uranus and Neptune fell under the gravitational control of Jupiter and Saturn (Brunini and Fernández 1999), so the latter two planets were responsible for the ejection of most of the residual planetesimals of the region of the jovian planets. Since most of the scattering by Uranus and Neptune occurred when the planets were near their final masses, had their formation time scales been longer than $\sim 10^8$ year, most of their residual bodies would have reached the Oort cloud region when the solar system had already departed from its natal environment. Numerical models that consider the solid–gas accretion of Uranus and Neptune (Pollack *et al.* 1996) and the non-negligible amounts of hydrogen and helium in their envelopes argue in favor of formation time scales considerably shorter than 10^8 year.

Brunini and Fernández (1999) recently considered the formation of Uranus and Neptune in the zone of the outer planets and the scattering of the residual planetesimals. From their study, three conclusions can be drawn of relevance for our present discussion:

1. The accretion of the outer planets was an inefficient process which required an initial mass 2–3 times larger than the combined masses of Uranus and Neptune.

2. Jupiter and Saturn were responsible for the ejection of $\sim$95% of the residual material of the accretion zones of Uranus and Neptune ($\sim$75% for Jupiter and $\sim$20% for Saturn). Only the remaining $\sim$5% was directly ejected by Uranus or Neptune.

3. The time scale of the accretion process of Uranus and Neptune and the scattering of residual material from their accretion zones is very short, of a few Myr, which might support the idea that it was coeval with the Sun still in its natal environment.

Fernández (1997) showed that a core of comets in tightly bound orbits with a radius of a few 10^3 AU would be the result of the perturbing action of a dense galactic environment on scattered planetesimals. Yet, Fernández's derivation was based on very simple analytical expressions, so a more rigorous treatment seems to be necessary. Gaidos (1995) also considered the formation of a transient Oort cloud of radius $\sim$3000 AU if the Sun was in a dense galactic environment, but he argued that it was disrupted by the very same strong external perturbers that formed it. An alternative mode of formation of an Oort cloud in a dense galactic environment was recently presented by Eggers *et al.* (1997), who considered the early Sun to be within an open cluster where swarms of intracluster comets were also produced by other cluster stars. In this scenario the Oort cloud was assumed to come from the capture of intracluster comets by the early Sun.

The aim of the present study is to test the hypothesis of formation and survival of a core of tightly bound comets around the early Sun, in a dense galactic environment, by means of numerical simulations that avoid some of the simplifications adopted in Fernández's (1997) work.

2. THE MODEL

We have made numerical simulations considering the early Sun in an environment much denser than the current one. The Sun was assumed to be formed together with other stars in a cluster with an initial density of: (1) 25 stars pc^{-3} ("dense star cluster") or (2) 10 stars pc^{-3} ("loose star cluster"). Furthermore, in most of the runs the Sun was assumed to be embedded in a condensed region of a molecular cloud of uniform density 10^5 H_2 cm^{-3} (in a few cases 3×10^4, or 10^4 H_2 cm^{-3}) of spherical shape (the "placental" gas), which is assumed to be the source of the Sun and the other cluster stars. We have also made some runs for a very dense star cluster of 100 stars pc^{-3} ("superdense star cluster") and some runs without the placental gas to check its dynamical influence on the formed Oort cloud. The relative

velocity between the Sun and other cluster stars was assumed to be 1 km s^{-1}.

The perturbation on the perihelion distance, δq, of a body at a distance r to the Sun caused by the tidal force of the placental gas acting during a time Δt was computed as (Fernández 1997)

$$\left(\frac{\delta q}{q}\right)_{\Delta t} = \frac{4\sqrt{2}\pi}{3}\,\frac{G\rho_c r^2 \cos\gamma \sin 2\eta \Delta t}{(GM_\odot q)^{1/2}}, \qquad (1)$$

where $\rho_c = 10^5$ H_2 cm^{-3} is the density of the placental gas, γ is the angle between the plane containing the radius vector $\mathbf{r}$ and the center of the placental gas and the plane containing the body's orbit, and η is the angle between $\mathbf{r}$ and the direction from the Sun to the center of the placental gas. The direction to the center of the placental gas was taken at random at the start of each run. The angles γ and η were computed taking instead of $\mathbf{r}$ the aphelion direction which can be derived very easily from the angular orbital parameters of the test body. In this regard we note that the aphelion direction is very close to that of $\mathbf{r}$ for near-parabolic orbits when $r \gg q$. The placental gas was assumed to act unchanged for (in most cases) 10^7 year, after which it dissipated instantaneously. Such a lifetime of $\sim 10^7$ year is compatible with observations of young star clusters embedded in dense cores of molecular clouds (Lada *et al.* 1996). The gas density drops with time, so the density of H_2 molecules may be much lower at 10^7 year. The gas effect may be overestimated, but, as we will show later, it has little dynamical effect on comets scattered by Uranus and Neptune. For comets scattered by Jupiter and Saturn (cases A and B) we also made some runs without gas and others with less dense gas and/or shorter lifetimes.

The perturbations caused by other cluster stars on the body were computed by integrating numerically each star passage in the frame of the three-body problem: Sun–cluster star–test body (for more details, see Brunini and Fernández 1996). A mass of 1 $M_\odot$ was assigned to each cluster star. It is to be noted that due to the very low encounter velocity (1 km s^{-1}), the impulse equation usually used to compute the star's perturbation on Oort cloud comets (e.g., Oort 1950, Rickman 1976, Weissman 1979, Fernández 1980) is in our case a very poor approximation. Oort's basic assumptions were that the star's trajectory remained unperturbed (i.e., a straight line in a heliocentric frame of reference) and that the comet was at rest during the encounter. These assumptions were reasonable for high encounter velocities, say 20–30 km s^{-1}, as is usually the case in the Sun's neighborhood at present. By contrast, we are now considering low encounter velocities for which the previous assumptions break down. In this regard, our simulations bring an improvement with respect to the analytical approximation by Fernández (1997).

We considered all the stellar encounters within a target radius of 3×10^4 AU. This value represents a reasonable compromise between a proper account of the dynamically more relevant encounters and their number (which increases with the square of the target radius), in order to avoid excessive computer times. As we will see in the next section, a radius of 3×10^4 AU is $\sim$3–5 times greater than the largest semimajor axes of bodies trapped in the Oort cloud. For closer star approaches the impulsive change on the comet's velocity goes as D^{-1}, where D is the distance of closest approach, while for more distant encounters, just of the order of 3–5 times the Sun–comet distance, it falls off more rapidly as D^{-2} (Brunini and Fernández 1996), which justifies the neglect of such more distant encounters.

The star cluster was assumed to lose stars with time until its complete dissolution at 10^8 year. This was simulated by computing a number density of cluster stars linearly decreasing at intervals of 10^7 year, from the initial value (100, 25, or 10 stars pc^{-3}) at $t = 0$, down to zero at $t = 10^8$ year.

We considered 42 samples of test bodies of varying sizes with initial perihelia within different ranges in the region of the jovian planets and low initial inclinations of either 0.1 or 0.2 radians. The low initial inclinations are justified on the basis that the test bodies are assumed to form in the protoplanetary disk from where they are scattered outward. The initial conditions of the different samples are described in Table I. We adopted two initial semimajor axes, $a_0 = 100$ AU, for bodies with smaller initial perihelion distances q_0 (bodies of Jupiter's zone), and $a_0 = 250$ AU, for bodies with q_0 between 8 and 30 AU (bodies of the zones of Saturn, Uranus, and Neptune). The initial orbits correspond to bodies scattered by the jovian planets from their accretion zones, whose aphelion distances are already too far away from the planetary region to characterize the orbits as "near parabolic" but, on the other hand, are still short enough to have been dynamically affected by external perturbers.

To analyze further the dynamical influence of the placental gas on comets scattered by Jupiter and Saturn (cases A and B), we made some additional runs (not indicated in Table I), for the case of a loose star cluster, $i_0 = 0.1$ radians, and smaller gas density and/or shorter lifetimes of 3×10^6, 10^6, 3×10^5, or 10^5 year.

The dynamical evolution of every test body was followed until one of the following end states: (1) the body was ejected along a hyperbolic orbit or placed in a very eccentric orbit with semimajor axis $a > 5 \times 10^4$ AU; (2) the semimajor axis of the body decreased below a certain threshold, in which case the body was assumed to return to the planetary region. We defined a treshold a_t that was $\sim$3–4 times greater than the initial q ($a_t =$ 26 AU for samples of the A and B series, and $a_t = 48$ AU for the remainder with the exception of E5 and E6, for which $a_t =$ 75 AU, and F5 and F6, for which $a_t = 100$ AU), in order to restrict our simulations of the evolution of bodies entering the planetary region to highly eccentric orbits.

Every time the test body entered the planetary region the probability of having a close encounter with any of the jovian planets was computed as

$$p = \frac{R_H^2}{2a_P^2 \sin i}, \qquad (2)$$

where $R_H = a_P(M_P/2M_\odot)^{1/3}$ is the Hill's radius of the sphere of influence of the considered jovian planet, M_P is its mass, and

TABLE I
Initial Conditions

Run	q_0 (AU)	i_0 (radians)	a_0 (AU)	Number of bodies	Star cluster	Gas
A1	4–6	0.1	100	5000	dense	yes
A2	4–6	0.2	100	5000	dense	yes
A3	4–6	0.1	100	2500	loose	yes
A4	4–6	0.2	100	2500	loose	yes
A5	4–6	0.1	100	5000	superdense	yes
A6	4–6	0.1	100	5000	superdense	no
A7	4–6	0.1	100	5000	loose	no
B1	6–8	0.1	100	2500	dense	yes
B2	6–8	0.2	100	2500	dense	yes
B3	6–8	0.1	100	2000	loose	yes
B4	6–8	0.2	100	2000	loose	yes
B5	6–8	0.1	100	2500	superdense	yes
B6	6–8	0.1	100	2500	superdense	no
B7	6–8	0.1	100	2500	loose	no
C1	8–12	0.1	250	2000	dense	yes
C2	8–12	0.2	250	2000	dense	yes
C3	8–12	0.1	250	2000	loose	yes
C4	8–12	0.2	250	2000	loose	yes
C5	8–12	0.1	250	2000	superdense	yes
C6	8–12	0.1	250	2000	superdense	no
C7	8–12	0.1	250	2000	loose	no
D1	12–16	0.1	250	1000	dense	yes
D2	12–16	0.2	250	1000	dense	yes
D3	12–16	0.1	250	1000	loose	yes
D4	12–16	0.2	250	1000	loose	yes
D5	12–16	0.1	250	1000	superdense	yes
D6	12–16	0.1	250	1000	superdense	no
D7	12–16	0.1	250	1000	loose	no
E1	16–22	0.1	250	500	dense	yes
E2	16–22	0.2	250	500	dense	yes
E3	16–22	0.1	250	500	loose	yes
E4	16–22	0.2	250	500	loose	yes
E5	16–22	0.1	250	1000	superdense	yes
E6	16–22	0.1	250	1000	superdense	no
E7	16–22	0.1	250	1000	loose	no
F1	22–30	0.1	250	1000	dense	yes
F2	22–30	0.2	250	500	dense	yes
F3	22–30	0.1	250	500	loose	yes
F4	22–30	0.2	250	500	loose	yes
F5	22–30	0.1	250	1000	superdense	yes
F6	22–30	0.1	250	1000	superdense	no
F7	22–30	0.1	250	1000	loose	no

a_P is its semimajor axis, and i is the orbital inclination of the test body. A random number $0 < z < 1$ was then taken, and if the condition $z < p$ was fulfilled for any of the four jovian planets, an encounter with it within the sphere of influence was assumed to occur. In this case the perturbation of the jovian planet on the body's orbit was computed in the frame of the two-body problem as the change in the direction of the planetocentric velocity vector at the entry and exit points of the sphere of influence (its modulus remained constant). Once the body left the Hill's sphere, the new heliocentric velocity was computed and hence the new orbital elements. This was assumed to be the only change suffered by the body's orbit during such a particular passage by the planetary region (this is because the perturbations by the other distant jovian planets became negligible in that case). We note that the two-body approximation is good in this case because we are considering high-velocity encounters between planets and bodies in near-parabolic orbits.

When $z > p$ for all the jovian planets, no close encounter occurred. In this case only the perturbation on the orbital energy x of the body (or reciprocal semimajor axis, $x \equiv 1/a$), as caused by the combined distant perturbations of the four jovian planets, was considered by taking at random a value δx from a Gaussian distribution of energy changes of standard deviation σ_x. For near-parabolic orbits the perturbations on the other orbital parameters are negligible as compared to the perturbation in x, which justifies taking them as constant during the body's perihelion passage. The standard deviation σ_x is a function of the body's perihelion distance q and inclination i. The adopted values of σ_x as a function of q and for different inclinations i are shown in Fig. 1 as derived by Fernández (1981). If a strong perturbation $\delta x > 5\sigma_x$ happened to be chosen, it was discarded and a new random δx was chosen on the basis that strong perturbations were already considered when $z < p$. We should note that the long tails in the x-distribution are associated with close planetary encounters (Everhart 1968). One may question whether the limit of $5\,\sigma_x$ is too crucial. Yet runs with $3\,\sigma_x$ gave no appreciable difference in the results.

When the test body was outside the planetary region, it was subject to external perturbers as described above. If the body's perihelion distance was raised above the planetary region, namely, when $q > 35$ AU, it was assumed to be trapped in the Oort reservoir and recorded as such. The later dynamical evolution of the body was followed until 10^8 year, or until ejection. It

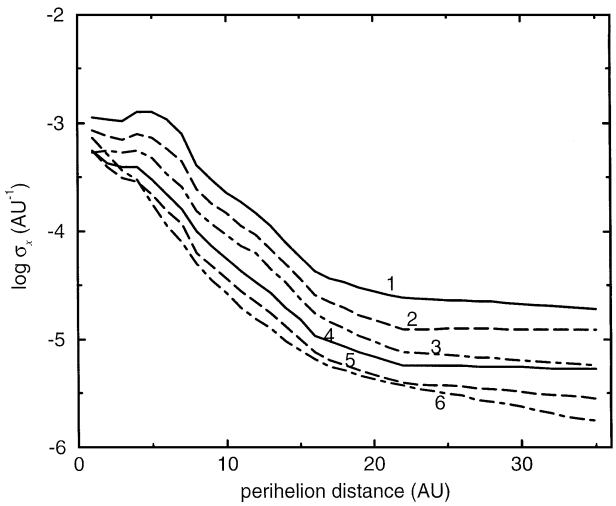

FIG. 1. Typical energy changes per perihelion passage of bodies in near-parabolic orbits, as given by the standard deviation of the δx-distribution of samples of test bodies with perihelion distances and inclinations within certain ranges, as a function of the perihelion distance and for different inclination ranges: $0 < i < 30^\circ$ (curve 1), . . . , $150^\circ < i < 180^\circ$ (curve 6).

was also possible that the external perturbers re-injected some bodies into the planetary region, in which case planetary perturbations started to act again.

3. THE RESULTS

Figure 2 shows plots of the perihelion distance versus semimajor axis of the bodies surviving at $t = 10^8$ year (most of them trapped in the Oort reservoir with $q > 35$ AU) for four different cases, two for a dense star cluster (A1 and E1), and two for a loose star cluster (A3 and E3). It is shown that most orbits are still very eccentric with most perihelion distances in the range $35 \lesssim q \lesssim 10^3$ AU and semimajor axes a in the range $500 \lesssim a \lesssim 10^4$ AU. It is noted that the bodies trapped in the Oort reservoir under a loose star cluster tend to be in somewhat less tightly bound orbits (on average greater a's). This is presumably due to the increase of the radius of the sphere of influence of the Sun as the density of neighbor cluster stars decreases, which allows it to keep more distant bodies gravitationally bound for the studied period.

We can compare the previous results with those obtained for the superdense cluster (A5, . . . , F5). The results shown in Fig. 3 clearly indicate that the effect of a stronger field of external perturbers is to form a smaller, more tightly bound core of comets. Most semimajor axes of trapped comets (again after 10^8 year) are in the range $10^2 < a < 10^3$ AU, independent of the initial q_0. The runs without the placental gas (A6, . . . , F6) lead to very similar results, showing that the dynamical influence of the placental gas is very minor in comparison with the cluster stars.

Figure 4 shows the histogram-distributions of reciprocal semimajor axes, $1/a$, for the same samples as in Fig. 2, considering only those bodies trapped in the Oort reservoir with $q > 35$ AU. The computed distributions show a spread of energies in the range $0 \lesssim 1/a \lesssim 10^{-3}$ AU^{-1}. By contrast, the observed distribution of original reciprocal semimajor axes of long-period comets, $(1/a)_{\rm orig}$ (i.e., those corrected by planetary perturbations), shows a narrow spike in the range $0 < 1/a < 10^{-4}$ AU^{-1} (the left bin of the panels in the figure), followed by a long tail

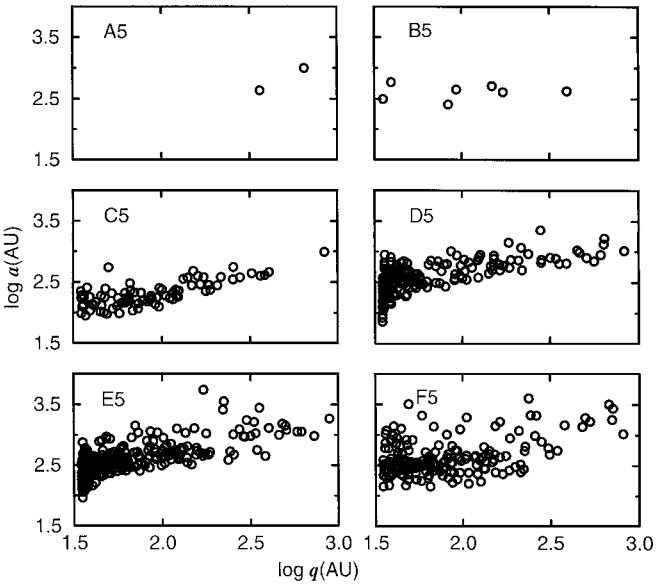

FIG. 3. Plots of semimajor axes versus perihelion distances of the test bodies surviving at $t = 10^8$ year for the samples A5, B5, C5, D5, and F5 corresponding to the superdense star cluster case.

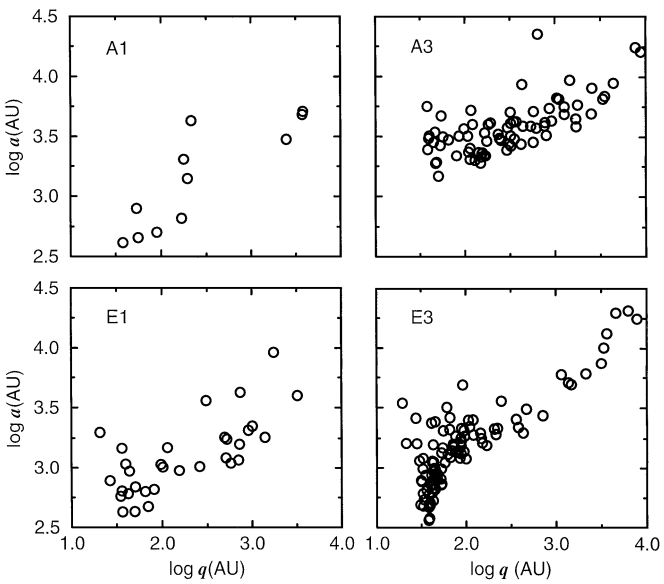

FIG. 2. Plots of semimajor axes versus perihelion distances of the test bodies surviving at $t = 10^8$ year for the samples indicated at the upper left corner of each panel.

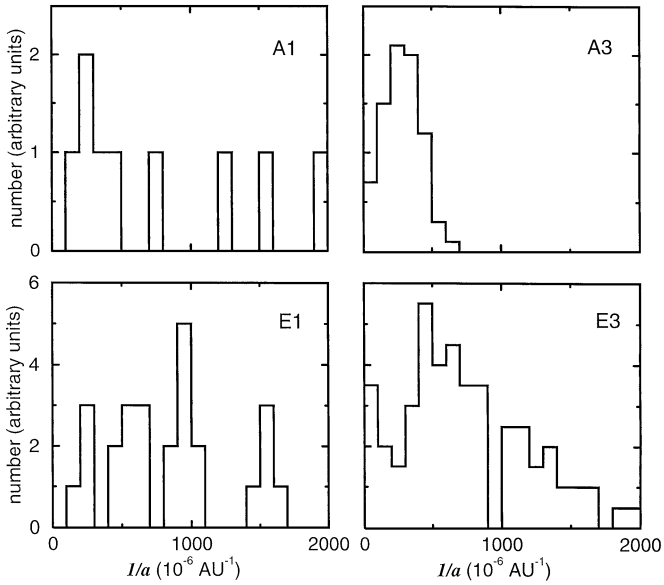

FIG. 4. Histogram-distributions of reciprocal semimajor axes of the test bodies trapped in the Oort reservoir at $t = 10^8$ year for the samples indicated at the upper right corner of each panel. Note that the width of a bin is 10^{-4} AU^{-1}, i.e., the width of the classical Oort comet cloud.

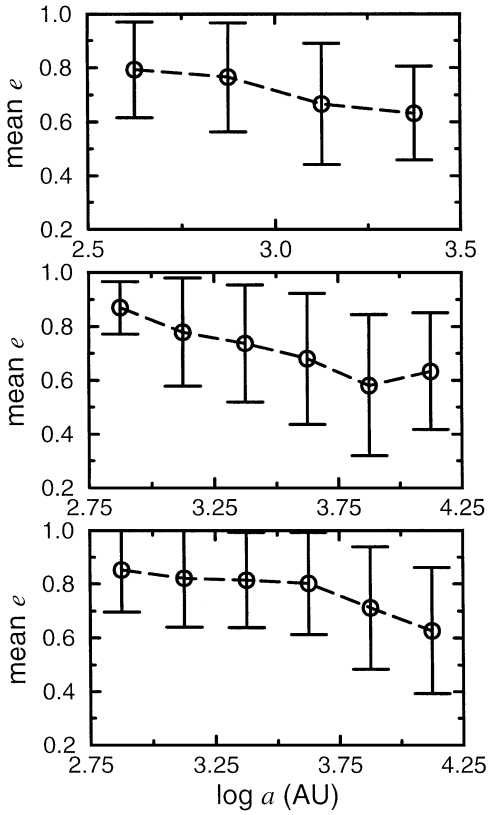

FIG. 5. Mean eccentricities of the bodies trapped in the Oort reservoir at $t = 10^8$ year with semimajor axes within ranges of 0.5 width (in logarithmic scale) for: (1) the samples A5, . . . , F5 corresponding to the superdense star cluster case (upper panel); (2) all the samples involving a dense cluster, A1, A2, B1, B2, . . . , F1, F2 (middle panel); and (3) all the samples involving a loose cluster, A3, A4, B3, B4, . . . , F3, F4 (lower panel).

of comets with larger binding energies (see Fig. 1 of Fernández 1997).

Figure 5 shows the mean values of the eccentricities of the bodies trapped in the Oort reservoir at $t = 10^8$ year for the superdense, dense, and loose star cluster cases. It is found that for smaller semimajor axes, bodies tend to keep high eccentric orbits ($\bar{e} \sim 0.85$–0.90), whereas for larger semimajor axes the mean eccentricity tends to $\sim 2/3$, which corresponds to a thermalized population (note that for a thermalized population the distribution of eccentricities follows the law $f(e) = 2e\,de$, see, e.g., Hills (1981)). The limiting semimajor axis, $a_{\rm L}$, for which the transition from a highly eccentric to a thermalized population depends on the number density of stars within the cluster. For the superdense star cluster case we find $a_{\rm L} \sim 10^3$ AU, while for the loose star cluster case we find $a_{\rm L} \sim 5 \times 10^3$ AU.

Figure 6 shows the distribution of inclinations of the same bodies shown in Fig. 4. It is shown that many bodies already reach retrograde orbits under the action of external perturbers, though the orbital planes of the populations are still far from being fully randomized (a sine law distribution).

Figure 7 shows the fraction of bodies that are ejected to interstellar space or attain $a > 5 \times 10^4$ AU for some of the samples of

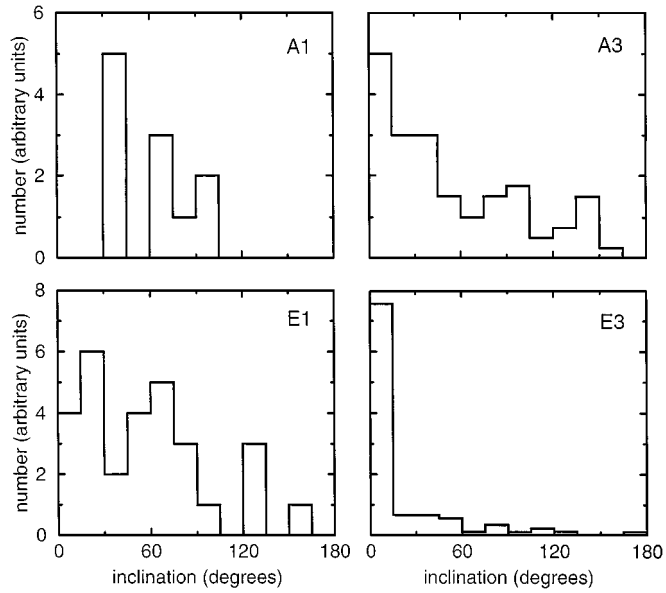

FIG. 6. Inclination-distributions of the test bodies trapped in the Oort reservoir at $t = 10^8$ year for the samples indicated at the upper right corner of each panel.

test bodies scattered from the regions of Jupiter, Saturn, Uranus, and Neptune with initial inclination 0.1 (upper panel) or 0.2 radian (lower panel). After a few Myr most bodies with perihelia in the Jupiter–Saturn region have already been ejected, whereas it

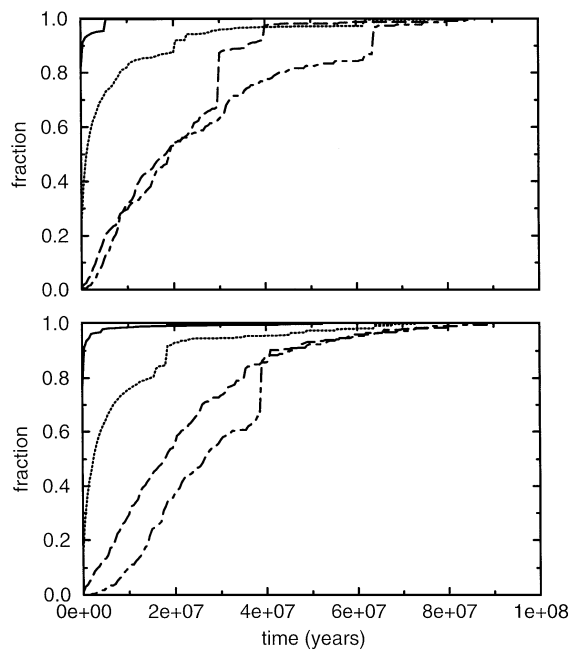

FIG. 7. Fraction of bodies that are ejected to interstellar space or attain $a > 5 \times 10^4$ AU, with respect to the total number of ejected comets at $t = 10^8$ year, as a function of time. The upper panel plots results for the samples A1 (solid curve), C1 (dotted curve), E1 (dashed curve), and F1 (dot-dashed curve). The lower panel idem for the samples A2, C2, E2, and F2.

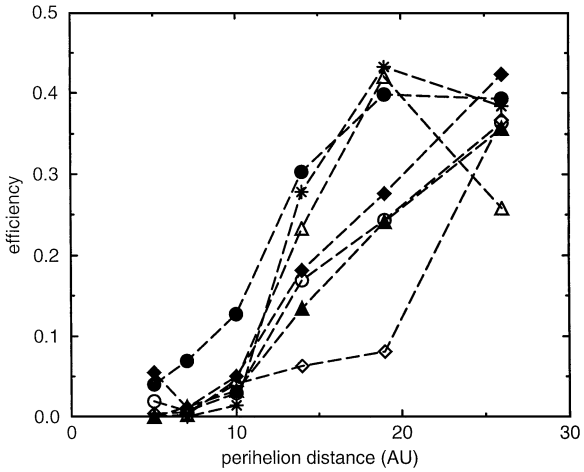

FIG. 8. Trapping efficiency in the Oort reservoir at $t = 10^8$ year as a function of the initial perihelion distance for all the samples shown in Table I. The symbols are for: A1, . . . , F1 (empty diamond); A2, . . . , F2 (empty circle); A3, . . . , F3 (filled diamond); A4, . . . , F4 (filled circle); A5, . . . , F5 (empty triangle); A6 , . . . , F6 (filled triangle); A7, . . . , F7 (stars).

takes ∼2–4 × 10^7 year for bodies with perihelia in the Uranus–Neptune region to be ejected. These dynamical lifetimes are of the same order as those involved in the trapping of bodies in the Oort reservoir. An inspection of the plots in both panels shows that dynamical lifetimes for ejection have only a little dependence on the initial inclination. The sudden jumps observed in the fractions of ejected bodies reflect the occurrence of strong perturbations of the inner core of the Oort cloud caused by very close stellar passages.

Figure 8 shows the trapping efficiency in the Oort reservoir at $t = 10^8$ year for all the studied samples. The trapping efficiency is defined as the ratio $N_{\rm oort}/(N_{\rm oort} + N_{\rm hyp} + N_{\rm pla})$, where $N_{\rm oort}$ is the number of comets trapped in the Oort reservoir at $t = 10^8$ year, $N_{\rm hyp}$ is the number of ejected comets, and $N_{\rm pla}$ is the number of comets that return to the planetary region. We found a strong dependence on the initial perihelion distance and inclination of the bodies, and also on the number density of the star cluster within which the Sun was assumed to form. Bodies with higher inclinations have in general a somewhat greater trapping efficiency, presumably due to the on-average smaller energy kicks that they experience in their passages by the planetary region. The trapping efficiency is of only a small percentage for bodies scattered from Jupiter's region; it increases to ∼3–10% for Saturn, to ∼10–40% for Uranus, and to ∼30–40% for bodies in the Neptune region. The trapping efficiency of Jupiter and Saturn is somewhat smaller for the superdense cluster cases.

We have also included the trapping efficiencies of comets for the cases of a loose cluster without molecular gas (series A7, . . . , F7). As shown, the influence of the molecular gas has a significant dynamical effect for the cases A and B, i.e., for those comets with smaller initial q. The trapping efficiency stays at a few percentage points when molecular gas is considered, but it drops to nearly zero when the gas is removed. We gave a close look at the problem of how the trapping efficiency of bodies scattered by Jupiter (cases A and B) varies with the density and lifetime of the natal molecular cloud. As mentioned, we made some additional runs, and the results are summarized in Table II. All the runs of Table II are for the case of a loose cluster. The second column shows the density of the molecular gas in relation to the standard density (10^5 H_2 cm^{-3}), the third column shows the lifetime of the molecular gas in Myr, and the fourth shows the trapping efficiency f_t. As shown, f_t strongly depends on the density and lifetime of the molecular cloud: it is about 5% for lifetimes of 1 Myr and densities 10^5 H_2 cm^{-3}, and it goes down to zero for cases without molecular gas. For a reasonable

TABLE II
Trapping Efficiency

Run	Dens.	Lifetime (Myr)	f_t
A11	1	1	0.053
B11	1	1	0.058
A12	1	0.1	1.6×10^{-3}
B12	1	0.1	1.2×10^{-3}
A13	0.1	1	8.8×10^{-3}
B13	0.1	1	5.2×10^{-3}
A14	0.3	3	0.026
B14	0.3	3	0.076
A15	0.3	0.3	0.012
B15	0.3	0.3	0.010

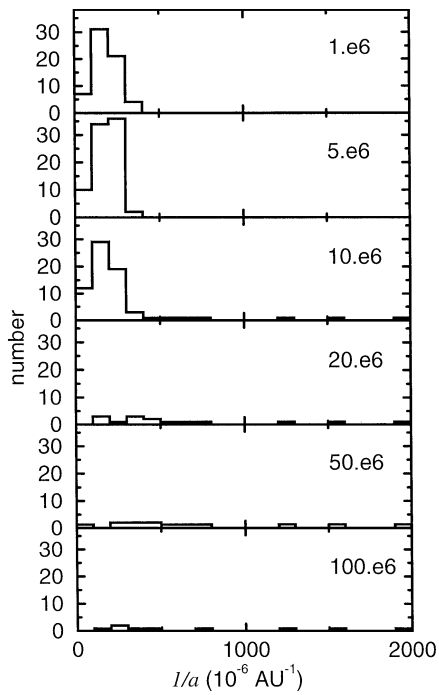

FIG. 9. Histogram-distributions of the reciprocal semimajor axes of those test bodies of the sample A1 trapped in the Oort reservoir at different times (given in years at the upper right corner of each panel).

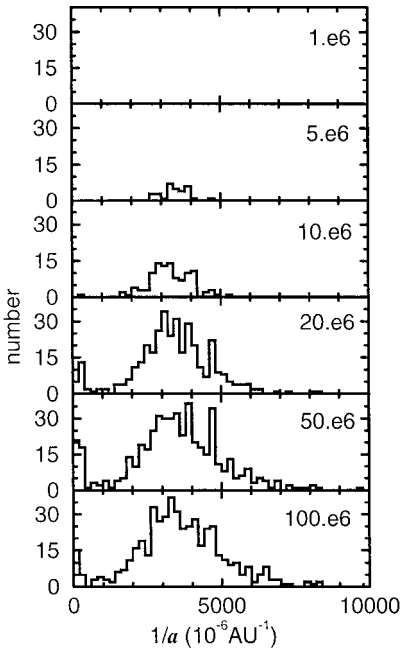

FIG. 10. Idem to Fig. 9 but for the sample F1.

combination of densities and lifetimes we should expect trapping efficiencies of the order of ∼1%.

For cases C, D, E, and F (i.e., $q > 8$ AU), the trapping efficiency is more or less the same for both cases, with or without molecular gas. Presumably, the reason for this is that the longer dynamical time scale for scattering makes most comets reach the Oort region when the placental gas has already dissipated, so in essence it makes no difference if the molecular gas was present during the first 10^7 year.

Figure 9 shows the time evolution of the distribution of reciprocal semimajor axes of the bodies trapped in the Oort reservoir for the sample A1 (bodies with initial perihelia in the Jupiter's region). A large number of bodies are initially trapped in the Oort reservoir at $t \sim 10^6$–10^7 year, but most of them—mainly those in more loosely bound orbits—are finally ejected due to the strong perturbations of cluster stars. This explains the low trapping efficiency of bodies of the Jupiter and Saturn region. The survivors in the Oort reservoir at $t = 10^8$ year (when the placental gas and cluster stars are supposed to have dissipated) are on average in more tightly bound orbits. The larger binding energies allowed such comets to withstand the strong external perturbations.

Figure 10 shows a distribution similar to that in Fig. 9, but for the case of bodies scattered by Neptune (sample F1). There are important differences in the dynamical evolution as compared to case A1. Comets start to get trapped in the Oort reservoir only after a few Myr, and they reach the maximum after a few tens Myr. The longer dynamical time scale illustrates by itself why the presence or not of molecular gas has negligible influence on the trapping efficiency. In any case, when most comets are trapped in the Oort reservoir (by the cluster starts), the molecular gas has already dissipated. Most comets trapped in the inner core of the Oort cloud have semimajor axes in the range $200 < a < 500$ AU; i.e., they are more tightly bound than in case A1.

Figure 11 shows how comets trapped in the Oort reservoir after 10^8 year would appear at a certain arbitrary time of their orbital periods, assuming that all of them are contained in the ecliptic plane. We have considered the three cases, dense, loose, and superdense star cluster. As seen, the radius of the formed comet core is finely tuned to the strength of the field of external perturbers, assuming it is constituted by stars formed in the same placental gas (as mentioned, the gas itself has a minor dynamical effect for most of the cases). In other words, the stronger the field of external perturbers, the more compact is the core of trapped comets. A loose star cluster will form a comet core of radius of

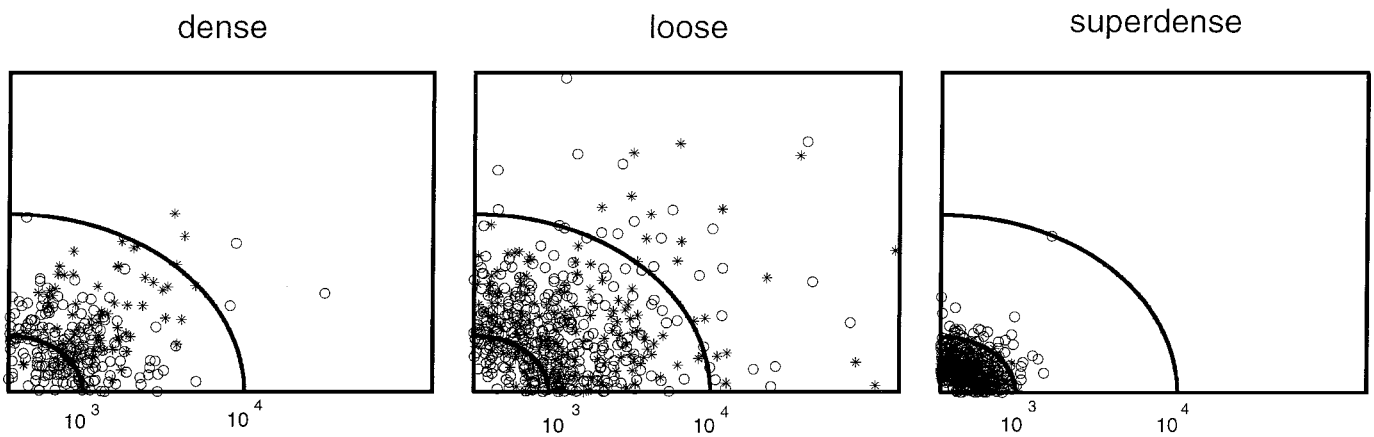

FIG. 11. A sketch showing how comets trapped in the Oort reservoir would appear distributed in the circumsolar space at a given time for the three cases of star cluster studied. The radii of the circles are expressed in AU. The symbols are for bodies from Jupiter–Saturn zones (series A, B, and C) (stars) and bodies from the Uranus–Neptune zones (series D, E, and F) (open circles).

a few 10^3 AU, while a superdense star cluster will form a more compact comet core of radius $\sim 10^3$ AU.

We do not find much difference between the space distribution of comets scattered from the Jupiter–Saturn zones (stars in Fig. 11) and those scattered from the Uranus–Neptune zones (open circles). In principle one should expect that comets scattered from the Jupiter–Saturn zones will meet a denser galactic environment due to their faster dynamical evolution, so they would be trapped in a more compact core. However, this is not seen in the figure, and the reason for this may be that the stronger kicks in energy received by comets passing by the Jupiter–Saturn zones more or less counteract the tendency of the stronger external field to trap comets of the Jupiter–Saturn zones in more tightly bound orbits.

4. EFFECTS ON AN EXTENDED KUIPER DISK

In a previous work (Brunini and Fernández 1996) we considered how the galactic environment constrains the size of an extended Kuiper disk and causes some dynamical stirring in its interior over the age of the solar system. We have now explored how a very strong field of external perturbers may affect the orderly, near-circular, and near-coplanar structure of the orbits of Uranus, Neptune, and Kuiper-disk objects. To this purpose we have made some numerical simulations of the dynamical evolution of extended Kuiper disks in dense galactic environments. We use the same program as before but without planetary perturbations, since our test bodies are far away from the planetary region. The r.m.s. changes in the relative energies $\Delta x/x$, eccentricities Δe, and inclinations Δi, after 10^8 year of samples of 200 test Kuiper-disk objects are shown in Table III. The test bodies are assumed to start in circular orbits with $i_0 = 0$ and the semimajor axis indicated in the first column of the table. The second column indicates the number density of the star cluster.

TABLE III
Dynamical Effects on Kuiper-Disk Bodies

a_0	$*/\mathrm{pc}^3$	$\log[\Delta x/x]$	$\log \Delta e$	$\log \Delta i$ (radians)	Fraction of survivors
250	10	−3.197	−2.551	−1.850	1.00
500	10	−2.914	−2.042	−1.572	1.00
750	10	−2.297	−1.302	−1.495	0.895
1000	10	−1.434	−0.427	−0.482	0.755
2000	10	−0.874	−0.395	−0.485	0.750
250	25	−2.969	−2.594	−1.845	1.00
500	25	−1.310	−0.867	−0.758	0.810
750	25	−0.965	−0.720	−0.453	0.785
1000	25	−0.859	−0.385	−0.377	0.510
2000	25	−0.481	−0.244	−0.145	0.450
250	100	−2.538	−1.670	−1.342	1.00
500	100	−0.891	−0.378	−0.657	0.755
750	100	−0.305	−0.342	−0.167	0.375
1000	100	0.113	−0.187	−0.008	0.275
2000	100	0.225	−0.174	0.071	0.015

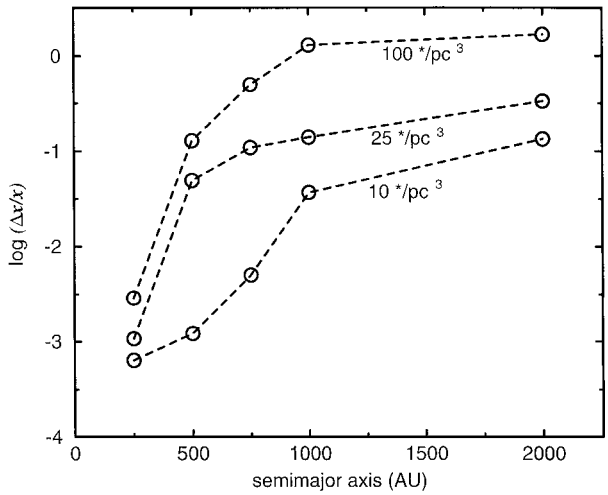

FIG. 12. The r.m.s. change in the relative energy as a function of the semimajor axis of Kuiper-disk bodies for the three densities of star clusters indicated beside each curve.

As before, the placental gas was included although its effect is very minor. The sixth column shows the fraction of Kuiper-disk bodies that survive at the end of the studied period.

The results suggest that the inner portions of the Kuiper disk—and therefore the orbits of Uranus and Neptune—could have withstood the strong external field, even in the case of a superdense star cluster, with very minor or negligible dynamical stirring. Yet, the external portions of a primordial extended Kuiper disk should have been completely disrupted, say for $a \gtrsim 500$ AU (Fig. 12). The disrupted portions of the extended Kuiper disk should have been replaced by the comet core. Of course, we are not discussing here how far away comet-sized bodies could form in an extended Kuiper disk. It might be possible that physical constraints, rather than dynamical ones, set the outer boundary of the Kuiper disk.

5. DISCUSSION

We find that a small but nonnegligible fraction of the bodies scattered by the jovian planets end up trapped in the Oort reservoir at the end of the studied period of $t = 10^8$ year. The efficiency of placing bodies in the Oort reservoir depends on the jovian planet that controls the dynamical scattering of bodies. It also depends on the orbital inclination of the scattered bodies and the density of stars and molecular gas in the galactic environment of the early Sun. Furthermore, the orbits of the trapped bodies are much more tightly bound than the orbits of the observed new comets, which also confirms the conclusion by Fernández (1997) that such bodies should form an inner core of the classical Oort cloud. It was also found that the radius of such an inner core is a function of the strength of the field of external perturbers, but it could be as small as a few 10^2 AU for a strong external field.

The timing of the scattering of bodies by the jovian planets and the dissolution of the natal galactic environment is essential to

evaluate the trapping efficiency in the Oort cloud. Gaidos (1995) considered the formation of an inner cloud of radius 100–300 AU from bodies scattered by Uranus and Neptune but finally ruled out this possibility on the basis of a too-long scattering time scale as compared to the lifetime of a stellar cluster. Yet Brunini and Fernández (1999) found very short time scales of accretion for Uranus and Neptune and scattering of the residual solid matter of their accretion zones. These results are more in agreement with their significant content of hydrogen and helium (e.g., Hubbard 1989), which suggests that they grew fast enough to be able to capture gas from the nebula before its dissipation. If this was the case, the scattering of bodies by Uranus and Neptune might have been coeval with the natal stellar cluster, thus allowing the formation of a comet core of the Oort cloud of no more than a few 10^2 AU radius. Of course, we can consider quite different scenarios of galactic environments leading to different comet cores of the Oort cloud. Our numerical study explores only some of the possible scenarios, but we consider them to be within realistic situations set by observational constraints.

If we assume, following Brunini and Fernández's (1999) results (see the Introduction), that about 50 $M_\oplus$ of the solid material of the Uranus and Neptune accretion zones was left unaccreted, this mass was finally ejected by the jovian planets according to the following contributions: Jupiter, $0.75 \times 50 = 37.5\,M_\oplus$; Saturn, $0.20 \times 50 = 10\,M_\oplus$; Uranus, $0.025 \times 50 = 1.25\,M_\oplus$; Neptune, $0.025 \times 50 = 1.25\,M_\oplus$ (we split the 5% contribution of Uranus and Neptune into equal parts). Jupiter and Saturn might have also ejected residual material from their own accretion zones (besides the material captured from the outer planets' zone) in a very short time scale, perhaps $\lesssim$1 Myr. If we assume that the amount of solid mass ejected by Jupiter and Saturn from their own accretion zones was of the order of their rock-icy cores of $\sim$15 $M_\oplus$ (e.g., Hubbard 1989) and make allowance for the fact that some material of the accretion zone of Saturn fell under the gravitational control of Jupiter, we can get ejected masses of $\sim$60 $M_\oplus$ for Jupiter, and of $\sim$20 $M_\oplus$ for Saturn.

If we now take for the jovian planets average fractions of the ejected material that is trapped in the Oort reservoir as discussed in the previous section (cf. Fig. 8), and the influence of the density and lifetime of the molecular gas for bodies scattered by Jupiter (cf. Table II), we finally obtain the total mass placed in the Oort reservoir:

- Jupiter: $60 \times 0.01 = 0.6\,M_\oplus$
- Saturn: $20 \times 0.03 = 0.6\,M_\oplus$
- Uranus: $1.25 \times 0.30 = 0.375\,M_\oplus$
- Neptune: $1.25 \times 0.40 = 0.5\,M_\oplus$.

It is possible that proto-Jupiter and proto-Saturn ejected material once they got masses of a few tens $M_\oplus$. In this case the fractions of bodies placed into the Oort reservoir by these two jovian planets could have been larger than those quoted above following their smoother random walk in energy space that favors trapping in the Oort reservoir.

Summing the above masses we get a total mass of about 2 $M_\oplus$. This mass is of the order of the estimated mass of the Oort cloud (Fernández 1982, Weissman 1983), derived from the observed frequency of passages of new comets and numerical models of the origin and dynamical evolution of comets formed in the outer planetary region. It is to be noted that Jupiter and Saturn become the main scatterers of matter to the Oort reservoir, though most of this material originally formed in the outer planetary zone. Material scattered by Uranus and Neptune after the star cluster dissipated probably ended up in the classical Oort cloud. Jupiter and Saturn might have scattered an amount of mass of their own accretion zones similar to the one computed above.

What was the later evolution of the bodies trapped in the inner core once the Sun left its natal environment? Strong perturbations during penetrating encounters with giant molecular clouds and very close stellar passages during the Solar System lifetime (4.6×10^9 year) might have produced a slow diffusion of bodies from the inner core to more loosely bound orbits. For a stellar flux of $\sim$7 stars Myr^{-1} through a circle of 1-pc radius (e.g., Fernández 1997) we should expect to have an encounter with a star within 3000 AU to the Sun every 600 Myr.

We showed that the orderly near-circular and near-coplanar structure of the orbits of Uranus and Neptune and Kuiper-disk bodies within distances of, say, $a \lesssim 200$ AU, can withstand a very strong field of external perturbers.

Our numerical simulations give support to the hypothesis of formation and survival of an inner core of comets in tightly bound orbits as a result of strong perturbations from a dense galactic environment. The semimajor axes of comets in the core might range between some hundreds and a few thousands AU. Its population and range of semimajor axes will depend on the particular characteristics of the galactic environment of the early Sun (density of molecular gas and mainly on the number density of neighbor stars) and on how long it could survive before dissipation. A very dense environment, for instance, if the Sun formed within a rich star cluster and stayed there for several 10^7 year, will favor a more centrally condensed core of comets. Such a core might have been left as a replenishment source of the classical Oort cloud through a slow diffusion process by penetrating encounters with giant molecular clouds and very close stellar passages. Hopefully, future improvements in telescopes and detectors will allow us to explore the circumsolar region at several hundreds AU to the Sun. At that moment the existence of such a core may be tested observationally, providing new insight into the early galactic environment of the Sun.

ACKNOWLEDGMENTS

We thank Eric Gaidos and Hal Levison who, as referees, made useful comments and criticisms that helped to improve the presentation of the results.

REFERENCES

Bally, J., L. Testi, A. Sargent, and J. Carlstrom 1998. Disk mass limits and lifetimes of externally irradiated young stellar objects embedded in the Orion nebula. *Astrophys. J.* **116**, 854–859.

Brunini, A., and J. A. Fernández 1996. Perturbations on an extended Kuiper disk caused by passing stars and giant molecular clouds. *Astron. Astrophys.* **308**, 988–994.

Brunini, A., and J. A. Fernández 1999. Numerical simulations of the accretion of Uranus and Neptune. *Planet. Space Sci.* **47**, 591–605.

Byl, J. 1983. Galactic perturbations of nearly parabolic cometary orbits. *Earth Moon Planets* **29**, 121–137.

Eggers, S., H. U. Keller, P. Kroupa, and W. J. Markiewicz 1997. Origin and dynamics of comets and star formation. *Planet. Space Sci.* **45**, 1099–1104.

Everhart, E. 1968. Change in total energy of comets passing through the Solar System. *Astron. J.* **73**, 1039–1052.

Fernández, J. A. 1980. Evolution of comet orbits under the perturbing influence of the giant planets and nearby stars. *Icarus* **42**, 406–421.

Fernández, J. A. 1981. New and evolved comets in the Solar System. *Astron. Astrophys.* **96**, 26–35.

Fernández, J. A. 1982. Dynamical aspects of the origin of comets. *Astron. J.* **87**, 1318–1332.

Fernández, J. A. 1997. The formation of the Oort cloud and the primitive galactic environment. *Icarus* **129**, 106–119.

Fernández, J. A. 1999. Comets: Clues to the formation of the Solar System and the early galactic environment. In *Planetary Systems—The Long View (9èmes Rencontres de Blois)* (L. M. Celnikier and J. Trân Thanh Vân, Eds.), pp. 119–124. Editions Frontieres.

Fernández, J. A., and A. Brunini 1998. Origin and evolution of the Oort cloud. In *Solar System Formation and Evolution* (D. Lazzaro, R. Vieira Martins, S. Ferraz–Mello, J. Fernandez, Eds.), ASP Conference Series Vol. 149, pp. 107–116. San Francisco.

Gaidos, E. J. 1995. Paleodynamics: Solar System formation and the early environment of the Sun. *Icarus* **114**, 258–268.

Heller, C. H. 1993. Encounters with protostellar disks. I. Disk tilt and the nonzero solar obliquity. *Astrophys. J.* **408**, 337–346.

Hills, J. G. 1981. Comet showers and the steady-state infall of comets from the Oort cloud. *Astron. J.* **86**, 1730–1740.

Hubbard, W. B. 1989. Structure and composition of giant planet interiors. In *Origin and Evolution of Planetary and Satellite Atmospheres* (S. K. Atreya, J. B. Pollack, and M. S. Matthews, Eds.), pp. 539–563. Univ. of Arizona Press, Tucson.

Lada, C. J., J. Alves, and E. A. Lada 1996. Near-infrared imaging of embedded clusters: NGC 1333. *Astron. J.* **111**, 1964–1976.

Lada, E. A., K. M. Strom, and P. C. Myers 1993. Environments of star formation: Relationship between molecular clouds, dense cores, and young stars. In *Protostars and Planets III* (E. H. Levy and J. I. Lunine, Eds.), pp. 125–162. Univ. of Arizona Press, Tucson.

Mottmann, J. 1977. Origin of the late heavy bombardment. *Icarus* **31**, 412–413.

O'Dell, C. R. 1998. Observational properties of the Orion nebula proplyds. *Astron. J.* **115**, 263–273.

Oort, J. H. 1950. The structure of the cloud of comets surrounding the Solar System and a hypothesis concerning its origin. *Bull. Astron. Inst. Neth.* **11**, 91–110.

Pollack, J. B., O. Hubickyj, P. Bodenheimer, J. J. Lissauer, M. Podolak, and Y. Greenzweig 1996. Formation of the giant planets by concurrent accretion of solids and gas. *Icarus* **124**, 62–85.

Reeves, H. 1978. The "Big Bang" theory of the origin of the Solar System. In *Protostars and Planets* (T. Gehrels, Ed.), pp. 399–426. Univ. Arizona Press, Tucson.

Reipurth, B., J. Bally, R. A. Fesen, and D. Devine 1998. Protostellar jets irradiated by massive stars. *Nature* **396**, 343–345.

Rickman, H. 1976. Stellar perturbations of orbits of long-period comets and their significance for cometary capture. *Bull. Astron. Inst. Czech.* **27**, 92–105.

Weissman, P. R. 1979. Physical and dynamical evolution of long-period comets. In *Dynamics of the Solar System* (R. L. Duncombe, Ed.), IAU Symp. 81, pp. 277–282. Reidel, Dordrecht.

Weissman, P. R. 1983. The mass of the Oort cloud. *Astron. Astrophys.* **118**, 90–94.